

Increased Expression of CD169 on Monocytes in Adult-Onset Kikuchi–Fujimoto Disease

Giacomo Malipiero ¹, Piernicola Machin ², Anna Ermacora ³, Chiara Pratesi ¹ , Antonino Carbone ^{2,4}, Desre' Ethel Fontana ¹, Kathreena Paul Vattamattathil ¹, Rita De Rosa ¹ and Paolo Doretto ^{1,*} 

¹ Clinical Pathology Unit, Ospedale Santa Maria degli Angeli, 33170 Pordenone, Italy; giacomo.malipiero@asfo.sanita.fvg.it (G.M.); chiara.pratesi@asfo.sanita.fvg.it (C.P.); desreethel.fontana@asfo.sanita.fvg.it (D.E.F.); kathreena.vattamattathil@asfo.sanita.fvg.it (K.P.V.); rita.derosa@asfo.sanita.fvg.it (R.D.R.)

² Pathology Unit, Ospedale Santa Maria degli Angeli, 33170 Pordenone, Italy; piernicola.machin@asfo.sanita.fvg.it (P.M.); antonino.carbone@asfo.sanita.fvg.it (A.C.)

³ Hematology Unit, Ospedale Santa Maria degli Angeli, 33170 Pordenone, Italy; anna.ermacora@asfo.sanita.fvg.it

⁴ Department of Pathology, Centro di Riferimento Oncologico-Istituto di Ricovero e Cura a Carattere Scientifico, National Cancer Institute, 33081 Aviano, Italy

* Correspondence: paolo.doretto@asfo.sanita.fvg.it

Abstract: Kikuchi–Fujimoto disease (KFD) is a rare, benign lymphoproliferative disease of uncertain origin that can mimic other inflammatory or clonal lymphoproliferative disorders. Given the lack of available blood biomarkers, diagnosis is based on the biopsy of an affected lymph node. In recent years, evidence has been mounting that a dysregulated type I INF innate immune response plays a pivotal role in the pathogenesis of the disease and might be a future therapeutic target. Nonetheless, laboratory assays measuring the expression of interferon alpha (INF α) and INF-stimulated genes (ISGs) are cumbersome and not widely available, limiting their use in clinical and translational research and encouraging the use of more convenient surrogate markers. In this study, a rapid flow cytometry assay detected increased levels of expression of CD169 (Siglec-1), an INF α -induced surface protein involved in innate immunity regulation, on circulating monocytes from two patients with KFD. Our results are in line with previous experiences and set the stage for a more extended investigation into the use of this assay in exploring the pathophysiology of KFD.

Keywords: Kikuchi–Fujimoto disease; monocyte; INF α ; SIGLEC-1; autoimmunity



Citation: Malipiero, G.; Machin, P.; Ermacora, A.; Pratesi, C.; Carbone, A.; Fontana, D.E.; Vattamattathil, K.P.; De Rosa, R.; Doretto, P. Increased Expression of CD169 on Monocytes in Adult-Onset Kikuchi–Fujimoto Disease. *Hemato* **2023**, *4*, 273–284. <https://doi.org/10.3390/hemato4030022>

Academic Editors: Carmelo Carlo-Stella and Robert Ohgami

Received: 5 May 2023

Revised: 27 July 2023

Accepted: 12 September 2023

Published: 15 September 2023



Copyright: © 2023 by the authors. Licensee MDPI, Basel, Switzerland. This article is an open access article distributed under the terms and conditions of the Creative Commons Attribution (CC BY) license (<https://creativecommons.org/licenses/by/4.0/>).

1. Introduction

Kikuchi–Fujimoto disease (KFD), also known as histiocytic necrotizing lymphadenitis without granulocytic infiltration, was first described in young Japanese females in 1972 [1,2] and is a rare, benign lymphoproliferative disorder with a definite histological pattern that is associated with a number of clinical scenarios of an inflammatory nature [3,4]. It is clinically characterized by self-limiting systemic symptoms (fever, weight loss, etc.) associated with localized tender lymphadenopathies, mostly of the cervical region. Nonetheless, extranodal involvement and complicated courses, in particular the subsequent or concomitant development of systemic inflammatory autoimmune diseases (SIADs) and/or hemophagocytic lymphohistiocytosis (HLH), have been recognized [4,5].

Pathologically, KFD is characterized by the paracortical proliferation of lymphocytes and immunoblasts, infiltration by histiocytes with characteristic crescent-shaped nuclei (Kikuchi's cells) and plasmacytoid dendritic cells (pDCs), the disruption of the follicular dendritic cell (FDC) meshwork and massive apoptosis with abundant nuclear debris [5–7]. The absence of granulocytic infiltration is a distinct hallmark that helps to differentiate KFD from other variants of necrotizing lymphadenitis.

While KFD is primarily supposed to reflect an aberrant cytotoxic-T-cell-mediated immune response to a variety of antigenic stimuli [8–10], the activation of the phagocyte mononuclear cell system has been proposed as a contributory mechanism. First, pathological investigations identified clusters of $\text{INF}\alpha$ -producing pDCs as specific histology-based diagnostic markers of KFD [8,11,12]. Next, gene expression studies in KFD histological samples showed that the molecular network in KFD is primed via the upregulation of ISGs [13]. Whether and how circulating myeloid cells are involved in this inflammatory *milieu* is under-investigated, although it is of potential interest for the identification of diagnostic/prognostic disease biomarkers.

The flow-cytometry-based measurement of sialic-acid-binding Ig-like Lectin 1 (SIGLEC-1, CD169), a surrogate marker of $\text{INF}\alpha$ activity, on the surfaces of monocytes has been the focus of increasing attention as a more convenient and rapid means of assessing $\text{INF}\alpha$ signaling in both sterile inflammatory and infectious viral diseases, including COVID-19 [14–18]. We herein provide evidence that circulating monocytes from two adult patients with biopsy-proven KFD exhibit increased surface expression of CD169. The pathophysiological implications of these findings are discussed.

2. Material and Methods

2.1. Flow Cytometry Evaluation of Monocyte CD169 Expression

To study the expression of CD169 on monocytes, we adopted a recently described one-step procedure proposed by Bougoin et al. to help differentiate bacterial versus viral infections in an acutely febrile patient based on a whole-blood flow cytometry assay combining the measurement of CD64 on neutrophils (which are increased in bacterial infections) and the measurement of CD169 on monocytes (which are increased in viral infections) [19,20]. Briefly, 10 μL of an EDTA-whole blood sample was simultaneously lysed with 500 μL of VersaFix lysing solution (Beckman Coulter, Hialeah, FL, USA) and stained with 5 μL of CD45KO and 10 μL of an IOTest Myeloid Activation antibody cocktail (Beckman Coulter) containing three markers: anti-CD169-PE (clone 7-239), anti-CD64-PB (clone 22) and anti-HLA-DR-APC (clone Immu357). After 15 min of incubation at room temperature in the dark, the samples were directly analyzed on a three-laser, ten-color Navios EX flow cytometer (BeckmanCoulter) according to a compensation-free protocol, and a further analysis was conducted using Kaluza Version 2.1.1 software (BeckmanCoulter).

For data analysis, leukocytes were gated using the side scatter (SSC) channel vs. the positive cluster of differentiation (CD45). Monocytes and lymphocytes were then identified on the basis of an SSC/CD64 dot plot as intermediate SSC/CD64⁺ and low SSC/CD64⁻, respectively. The mean fluorescence intensity CD169 (MFI CD169) was measured in each population. The results were expressed as the ratio of CD169 MFI values between monocytes and lymphocytes (Figure 1a,b). As previously reported, a threshold value greater than or equal to 3.51 was used to discriminate patients with a viral infection [20]. This threshold was also confirmed in 55 healthy controls who were enrolled from our institution, with median age of 53 (range: 30–69) years and with a predominance of males (66%). In this cohort, the mean MFI CD169 ratio was 2.2 ± 0.74 (the median + two standard deviations) (Figure 1c). As positive controls, we assessed the expression of mCD169 in 30 consecutive patients with a confirmed diagnosis of COVID-19 who were age-matched with our KFD cases and admitted to our Emergency Department from 15 December 2021 to 5 March 2022. In this cohort, all patients except one showed an MFI CD169 ratio above the threshold, with an overall mean of 16.2 ± 9.6 (mean \pm sd) (Figure 1d).

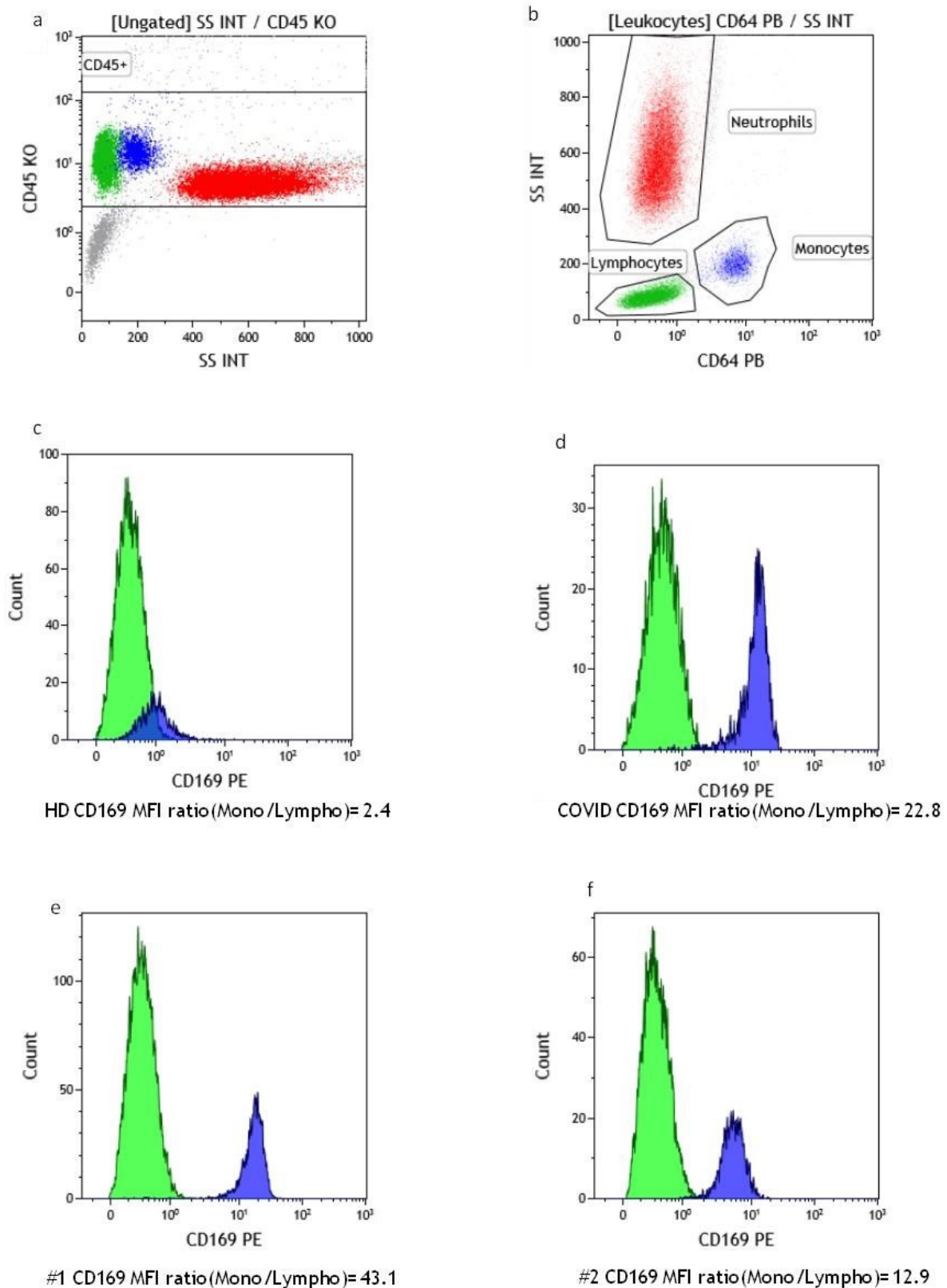


Figure 1. Gating strategy: leukocytes were gated using the side scatter (SSC) channel vs. CD45 (a). Monocytes and lymphocytes were then identified as intermediate SSC/CD64⁺ and low SSC/CD64⁻, respectively (b). Representative histograms of the mean fluorescence intensity of CD169 (CD169MFI) in lymphocytes (green) and monocytes (blue) in healthy donors (c), COVID-19 patients (d), case #1 (e) and case #2 (f). The MFI ratios are depicted.

2.2. Suspensions and Biopsy Immunophenotyping via Flow Cytometry

The lymph node specimens were prepared in the standard manner used for the routine clinical immunophenotyping of tissues in our laboratory. Briefly, the tissue was finely minced in 3 to 5 mL of RPMI using a scalpel. The homogenate was then filtered through a 40 µm filter, centrifuged at 550 × g for 10 min, washed with PBS containing 1% BSA and then resuspended in an appropriate cell concentration (2–20 × 10⁹ cells/L) in RPMI-1640. The biopsy specimens were washed twice with PBS/BSA, spun at 550 × g for 5 min and resuspended to an appropriate cell concentration. A 100 µL aliquot of specimen was prewashed to avoid plasma–serum protein interferences, and red blood cells were lysed with 1 mL of a 1 × IOTest3 lysing solution for 15 min and washed with PBS/BSA. After the supernatant was removed, the sample was stained using a ClearLLab LS cell tube (Beckman Coulter), according to the manufacturer’s instructions. A ClearLLab LS cell tube contains dry, pre-mixed reagents including 12 antibodies used to identify and characterize cells expressing the Kappa/CD8 (FITC), Lambda/CD4 (PE), CD19 (ECD), CD56 (PC5.5), CD10 (PC7), CD34 (APC), CD5 (APC-A700), CD20 (APC-A750), CD3 (Pacific Blue) and CD45 (Krome Orange) antigens via flow cytometry. After using a strong vortex to detach the antibodies, the mix was incubated in the dark at room temperature for 15 min and washed with PBS/BSA. After the removal of the supernatant, at least 50,000 events were acquired using the Navios EX. The stained samples were acquired using the Navios EX cytometer (Beckman Coulter), and a further analysis was conducted using Kaluza Version 2.1.1 software (Beckman Coulter). Clonal populations, if present, were identified and immunophenotyped. If aberrant T-cell populations or plasma cell populations were suspected, a further investigation with the appropriate extended panels was performed.

2.3. Pathological Analysis

Formalin-fixed, paraffin-embedded lymph nodes and blocks were retrieved from the files of the Pathology Unit of Pordenone Hospital. Sections measuring 3 mm thick were cut from the paraffin blocks and stained with hematoxylin and eosin (H&E), Giemsa, periodic acid–Schiff and AFB. Further sections were used for immunohistochemistry, which was performed by applying the following antibodies: CD20 (L26, Roche/Ventana, Oro Valley, AZ, USA), CD3 (2GV6 Roche/Ventana), CD4 (PS35, Roche/Ventana) CD8 (SP57, Roche/Ventana), CD163 (MRQ-26, Roche/Ventana), CD1a (EP3622, Roche/Ventana), CD30 (BERH2, Roche/Ventana), CD138 (B-A38, Roche/Ventana), CD56 (MRQ-42, Roche/Ventana), CD117 (EP10, Roche/Ventana), tryptase (G3, Roche/Ventana), ERG (EPR3864, Roche/Ventana), cyclin D1 (SP4-R, Roche/Ventana), CD34 (QBEnd/10, Roche/Ventana), CD31 (JC70, Roche/Ventana), Ki67 (30-9, Roche/Ventana), panCKAE1/AE3 (PCK26, Roche/Ventana) and CD68 (PGM-1, Diagnostic biosystem). The antibodies were dispensed on a BenchMark Ultra HD immunostainer and detected via the alkaline phosphatase–anti alkaline phosphatase technique or the streptavidin–biotin–peroxidase complex method. Antigen retrieval was performed according to the protocols used in our laboratory. In all instances, internal positive and negative controls were used to assess the reliability of the results.

2.4. Case Reports

2.4.1. Case 1

A 26-year-old otherwise healthy man of Indian origin was hospitalized in September 2021, reporting a 45-day-long history of undifferentiated fever, generalized malaise and weight loss (–12.5 kg in three months). He had moved from India to Italy 5 years earlier and did not report recent travels abroad. His history did not suggest any exposure to environmental or occupational risk factors. A physical exam was non-contributory. A complete blood count and routine biochemistry panels were unremarkable except for mild increases in C-reactive protein (CRP) (1.3 mg/dL, n.v. < 0.5) and lactate dehydrogenase (247 U/L, n.v. 100–240) and the presence of activated lymphocytes on a peripheral blood smear. An X-ray scan of the chest did not reveal any inflammatory changes. Flow

cytometry was conducted on circulating monocytes and showed a markedly increased expression of CD169 on their surfaces (ratio: 44.7), suggesting a possible viral etiology (Figure 1e). Nonetheless, the patient had non-reactive serology for acute Epstein–Barr virus, cytomegalovirus, herpes simplex virus, and human immunodeficiency virus infections and reactive serology for past exposures to EBV and CMV. He had received the first dose of an mRNA-based anti-SARS-COV-2 vaccine at the beginning of August, so serology for SARS-CoV-2 was positive but direct antigen and nucleic acid tests on nasopharyngeal swabs were negative. An ANA indirect immunofluorescence screening of Hep-2 cells and serology for *Bartonella henselae* and *Toxoplasma* were non-reactive. An INF γ release assay for *Mycobacterium tuberculosis* was negative. Direct microbiological investigations, including blood and urine cultures, were also negative. A whole-body computed tomography (CT) scan was obtained which demonstrated bilateral neck and axillary lymphadenopathies of 3–4 cm in diameter, one of which was excised for diagnostic purposes. A histological examination showed foci of necrosis with abundant karyorrhexis, foamy histiocytes and rare immunoblasts in the absence of neutrophil granulocytes (Figure 2). A search for acid alcohol-resistant mycetes and bacilli yielded negative results (Giemsa, PASD and AFB). The morpho-immunophenotypic findings were consistent with histiocytic necrotizing lymphadenitis. Flow cytometry immunophenotyping did not support evidence of hematological malignancies since the analysis did not display a light chain restriction nor an aberrant expression of B or T markers.

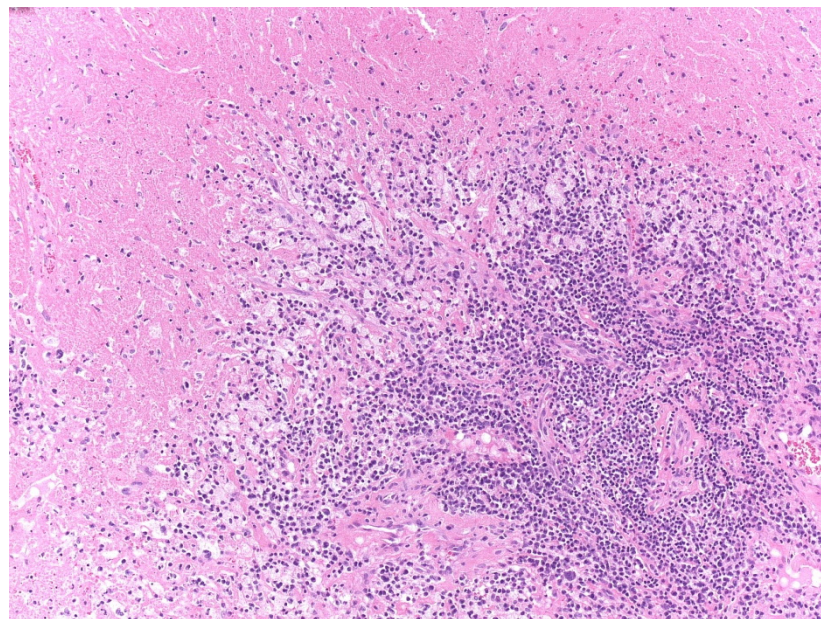


Figure 2. Case 1 Axillary lymphonode biopsy: the upper left part of the field is mainly marked by apoptotic necrosis, the central part by the infiltration of foamy histiocytes and the lower right part by residual lymphonode parenchyma (10 \times ; H&E).

Oral corticosteroids (prednisone 1 mg/kg) were initiated with a prompt resolution of symptoms and slowly tapered until complete suspension without the recrudescence of clinical symptoms in the following months.

2.4.2. Case 2

A 29-year-old man of Indian origin was admitted to the hospital at the end of April 2021 for generalized seizures. In the previous 60 days, he had been admitted to the Emergency Department (ED) twice, reporting fever (up to 39.4 °C), tender lymphadenomegaly of the neck, anorexia, weight loss and odynophagia that scarcely responded to over-the-counter non-steroidal anti-inflammatory drugs. He had moved from India to Italy 19 years

earlier and did not report recent travels abroad. He was employed at a local furniture factory as a worker. His past medical history was non-significant. At both ED admissions, a chest X-ray showed mild bibasal interstitial attenuation. He had been treated with empiric antibiotic therapy and two short courses of an oral corticosteroid with partial and transient remissions of his symptoms. He had then undergone a neck echography which showed multiple bilateral nodal enlargements up to 1.2 cm in diameter with cortical thickening, and a chest CT scan revealed multiple supra-diaphragmatic nodal enlargements, splenomegaly (12.9 cm) and bibasal areas of ground-glass opacity in the lungs. The day before undergoing a scheduled nodal biopsy, the patient presented to the ED with worsening seizures which evolved into status epilepticus. He was intubated, admitted to the Intensive Care Unit and treated with a continuous infusion of sodium valproate. The results of a cerebrospinal fluid chemical analysis were unremarkable and the results of HSV, VZV and EBV polymerase chain reactions conducted using the cerebrospinal fluid were negative. A CT scan of the head was negative for acute stroke. An electroencephalogram showed signs of diffuse cortical suffering, while magnetic resonance imaging revealed an area of weak hyperintensity on long TR sequences in the left hippocampus. Dexamethasone (8 mg BID) was administered for suspected central nervous system localization of lymphoma.

A fine-needle biopsy from one axillary node was obtained the day after admission: pathological analysis showed extensive coagulative necrosis of the lymph node with numerous foamy histiocytes. Immunohistochemistry found no alteration of the expression of the tested antigens. The search for acid-alcohol-resistant mycetes and bacilli yielded negative results (Giemsa, PASD, and AFB). After three days of ventilatory mechanical support, the sodium valproate infusion was tapered down without a recurrence of epileptic seizures, and the patient was extubated and transferred to the Internal Medicine Unit on oral valproate (500 mg bid) and prednisone (1 mg/kg day). At the time of this admission, the available results of a biochemical investigation highlighted a mild increase in CRP (3.5 mg/dL) and a markedly increased expression of CD169 on blood monocytes (ratio 12.6) (Figure 1f), while the very same microbiological work-up did not reveal any viral etiology for case 1. A bronchoalveolar lavage was performed for microbiological screening, but this was inconclusive as well. Otherwise, an ANA indirect immunofluorescence screening on Hep-2 cells was positive at a 1/320 titer with a nucleolar pattern. An ENA screening (CLIA) was positive for anti-Scl70 (71, n.v. < 7 AU/mL). A line-blot immunoassay for systemic sclerosis and myositis-specific and myositis-associated antigens was performed and confirmed anti-Scl70 positivity. Rheumatoid factor, anti-neutrophil cytoplasm antigen IgG, anti-cardiolipin, anti- β 2 glycoprotein IgG and anti-onconeural and encephalitis-associated IgG antigens were undetectable. C3 and C4 were within normal ranges. Given the absence of gross manifestations of scleroderma, a capillaroscopy was performed which showed non-specific capillary abnormalities including irregular capillaries, neoangiogenesis, capillary ectasia and edema. A full work-up for SSc was performed without detecting the involvement of other organs. Pulmonary hypertension was not estimable on an echocardiogram since tricuspid regurgitation was absent. Even though the clinical and serological pattern was strongly suggestive for limited cutaneous systemic sclerosis (SS), a definite diagnosis could not be provided according to the EULAR 2013 classification criteria [21], and an axillary lymph node excision biopsy was performed in order to exclude an underlying clonal lymphoproliferative disease (Figure 3). A histological examination showed foci of necrosis with abundant karyorrhexis, histiocytes and rare immunoblasts in the absence of neutrophil granulocytes. The search for acid-alcohol-resistant mycetes and bacilli yielded negative results (Giemsa, PASD, and AFB). The morpho-immunophenotypic finding was consistent with histiocytic necrotizing lymphadenitis. Flow cytometry showed that the majority of gated cells were early apoptotic cells with low forward scatter and without the expression of any tested antigens, in agreement with the histopathologic and immunohistochemical findings; no signs of clonal lymphoproliferation were detected. To complete the hematological work-up, bone marrow cytology and biopsy were performed, showing no

abnormalities of myeloid, erythroid or megakaryocytic maturation; abnormal lymphoid infiltration and hemophagocytosis were not observed.

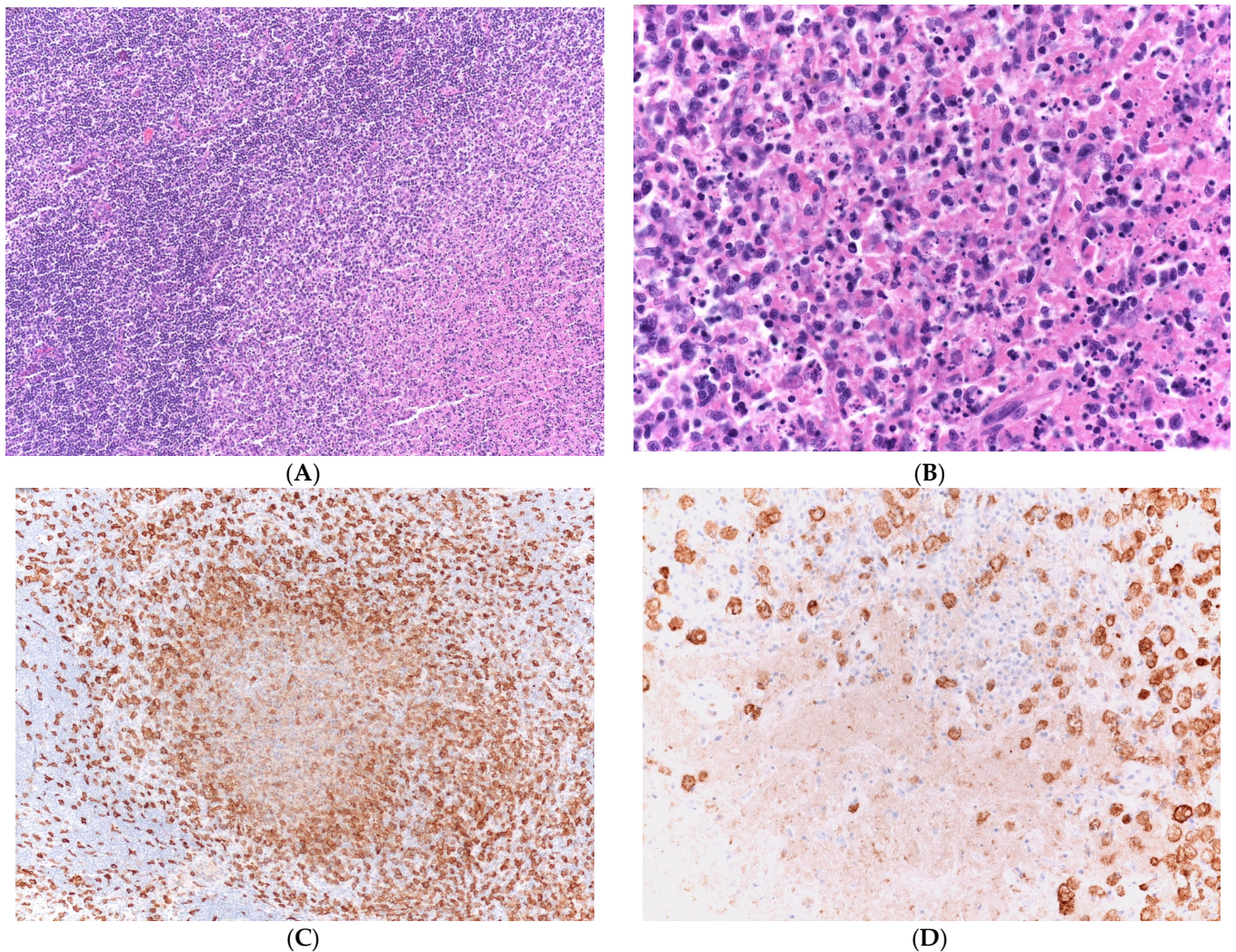


Figure 3. Case 2 axillary lymphonode biopsy. (A) The upper left part of the field is represented by normal lymphonodal parenchyma; the central part by histiocytic infiltration and the lower right part by necrosis (10×; H&E). (B) Particular of apoptotic histiocytic necrosis. (C,D) CD68 immunostaining. In (C), CD68⁺-cells surround an area of central apoptotic necrosis; in (D), CD68⁺-cells intermingle with lymphocytes at the periphery of an apoptotic area.

A conclusive diagnosis of KFD associated with unclassifiable connective tissue and interstitial lung disease was given. The pathological nature of central nervous system involvement was difficult to ascertain and was potentially consistent with either fever-induced epilepsy, SS-related encephalitis or KFD localization. Mycophenolate mofetil (1 g BID) was introduced. At a 3 month follow-up, the patient was subjectively asymptomatic, the lymphadenopathies had regressed and an MR image of the head was unremarkable. No new signs of scleroderma were reported, and a chest CT scan showed resolving bibasal ground-glass opacities. Nine months later, a repeated chest CT showed resolved ground-glass opacities with residual signs of reticular lung fibrosis. The patient is now being closely monitored for early signs of disease progression.

3. Discussion

We reported two cases of KFD that exemplify the clinical heterogeneity and diagnostic conundrums of this uncommon lymphoproliferative disease. KFD is a histiocytic necro-

tizing lymphadenitis that was first described in 1972 [1,2]. Its etiology is hypothesized to involve an aberrant interaction between antigenic stimuli and the host's response. In both of our patients, the most common infective causes of lymphadenopathy (mycobacterial disease, cat scratch disease, EBV, etc.) were excluded, but the list of pathogens implicated in KFD is periodically updated, and new pathogens have emerged for which diagnostic kits were not available at our Institution [22]. The administration of COVID-19 mRNA-based vaccines has been reported to trigger KFD, even with delayed onset [23], and might be implicated in case 1, although subsequent scheduled dose administrations had apparently no effect on disease activity. An association with autoimmunity has been widely described in KFD, but the precise physiopathological link is controversial [24,25]. The serological and clinical phenotype of the patient in case 2 was highly suggestive of SS, in spite of the fact that the classification criteria according to EULAR 2019 [21] were not fully met. In this instance, interstitial lung disease was interpreted as a *bona fide* manifestation of systemic autoimmunity, and a lung biopsy was considered not worth the risk for further case definition and not influent on treatment decision making. It should be noted, however, that lung involvement in KFD has been reported, so we could not definitely exclude a lung localization of KFD, though it is rather unlikely and unusual [26]. The same holds true for limbic encephalitis presenting as status epilepticus, which has been associated with both KFD and systemic sclerosis [27,28].

Even though the clinical picture, young age, ethnic background, exposure to a potential trigger and associated autoimmunity may favor a diagnosis of KFD, an invasive investigation is required in most cases to confirm the clinical suspicion and exclude a malignant lymphoproliferative disease. The pathological differential diagnosis is broad and mainly includes SIADs-associated lymphadenopathy (mainly systemic lupus erythematosus), non-Hodgkin lymphomas and, less frequently, infectious lymphadenitis (tuberculosis, histoplasmosis, leprosy, cat-scratch disease, syphilis, *Yersinia enterocolitica* bacterial infection, HSV and infectious mononucleosis) [29–32]. In both our cases, necrotizing lymphadenopathy was pathologically confirmed and mostly consistent with the xanthomatous phase of KFD. No evidence of malignancy was found via flow cytometry and pathological analyses. In summary, these cases exemplify the protean clinical manifestations of KFD, the diagnostic challenges with clonal lymphoproliferations and its ambiguous pathobiological relationship with autoimmunity.

The expansion of the lymph node paracortical zone via the proliferation of sheets of large CD8⁺-cytotoxic lymphocytes is considered the most prominent feature of Kikuchi–Fujimoto lymphadenitis and is involved in tissue apoptosis [33,34]. Nonetheless, the mechanisms of CD8⁺ T-cell activation and the interplay between T-cells, histiocytes, pDCs and FDCs are incompletely understood [34–36]. Indeed, the upregulation of ISG has been consistently reported in KFD [8,11–13], suggesting INF-type-I-producing mononuclear phagocytes may trigger T-cell activation. While pDCs are supposed to be the main INF type I producers at the tissue level, circulating mononuclear and bone marrow myeloid cells have received less attention. A systematic study of blood and bone marrow changes in a series of KFD patients demonstrated that a significant number of patients had single or multiple cytopenias of central origin (particularly those evolving into HLH), while a smaller fraction presented low-degree leukocytosis, thrombocytosis or atypical lymphocytes (for these patients, bone marrow studies were not available) [37]. Contrary to these findings, a recent PET/CT scan study showed that 50% (20/40) of KFD patients had splenomegaly and spleen hypermetabolism, 75% (30/40) had hypermetabolism of the central and peripheral bone marrow and they all exhibited features of myeloid hyperplasia on bone marrow smears [38]. A single study dating back to 2013 demonstrated the upregulation of ISG in the circulating phagocytes of KFD patients [39]. Taken together, these findings suggest that the myeloid compartment is involved in KFD, raising the question as to whether myeloid changes are secondary to the local production of cytokines in the lymph node or, conversely, whether activated blood-borne phagocytes primarily colonize peripheral tissues, where they trigger a necrotizing, histiocyte-rich lymphoproliferative reaction pattern. With respect

to this, it is noteworthy that KFD has been reported in VEXAS syndrome, a primary bone marrow disease, due to the somatic mutations of hematopoietic progenitors with both myelodysplastic and autoinflammatory features [40,41].

CD169, a member of the Siglec family, is expressed on the surfaces of specific subsets of macrophages, precursor monocytes and DCs. It contributes to cell–cell adhesion and cell–pathogen interactions since it has high affinity for $\alpha 2$ 3 glycosyltransferase and glucosidase and communicates with other immune cells by binding to other cell-surface polysaccharides (e.g., CD43 on T cells) [42,43]. The expression of CD169 is induced on monocytes upon stimulation via type I INF pathways [14] and is associated with higher co-expression levels of co-stimulatory and HLA molecules, suggesting an increased activation state [44]. We herein provided evidence that circulating monocytes from two KFD patients exhibited increased levels of expression of SIGLEC-1 (CD169), a master ISG. Our findings are consistent with those of a recently published paper on a cohort of pediatric KFD patients [45], although different flow cytometry protocols were used, making a direct comparison of the results unreliable. While a direct pathogenic role of CD169 could not be demonstrated, there is evidence that this surface protein might be biologically relevant in KFD. Studies have shown that nodal sinus CD169⁺-macrophages inform pDC physiology [46] and CD169-monocytes gain CD8⁺-cell-activating properties [44]. Moreover, a type I INF molecular signature is increasingly recognized in SIADs, and experimental models have proposed that the loss of peripheral tolerance in systemic connective tissue diseases is consequent to functional abnormalities in phagocyte system physiology, namely a release of INF α due to aberrant mitochondrial catabolism [47,48]. The hyperexpression of CD169 on monocytes has also been associated with SS-ILD [49], and animal models of SS-ILD have demonstrated that monocytes trigger lung inflammation by interacting with anti-topoisomerase antibodies [50]. Unfortunately, we could not evaluate the expression of SIGLEC-1 in circulating dendritic cells, which were excluded by our gating strategy, or in the patients' lymph node samples to define its expression in tissue pDCs and histiocytes. Even though we could not provide evidence of a pathophysiologic link between the circulating activated monocytes and histological changes, it is tempting to speculate that in KFD, the activation of the phagocyte system orchestrates a range of functional derangements that might result in a loss of peripheral tolerance and superimposed systemic autoimmunity or macrophage activation syndrome.

In the absence of specific laboratory markers of KFD, carrying out CD169 flow cytometry on circulating monocytes might be useful for strengthening the clinical suspicion of KFD in the appropriate clinical context and to monitor disease activity or the response to anti-inflammatory therapy. Admittedly, we did not evaluate the expression of CD169 as a diagnostic or prognostic marker, for example, to monitor a response to steroid therapy and provide a correlative analysis of MFI values with disease severity, due to the limited number of patients and considering that the case 2 patient was already on steroid therapy when the flow cytometry assay was performed. Indeed, the upregulation of CD169 has been described in other inflammatory diseases [51,52] and may involve different subsets of mononuclear phagocytes with different, and even opposite, functional outcomes (conventional dendritic cells, pDCs, pre-DCs and M1 or M2 monocytes) in a disease-specific manner, lowering the specificity of the test. Whether specificity is at least retained for segregating inflammatory versus malignant lymphoproliferation will be a key investigative focus for the future. We only retrieved one study that showed that DLBCL is associated with a reduction in the number of CD169⁺-macrophages in affected tissues [53], while the phenotypic patterns of circulating blood cells are mostly unknown, particularly in histiocyte-rich variants of lymphoma.

Author Contributions: Conceptualization, G.M.; methodology, P.D.; validation C.P.; formal analysis G.M.; investigation P.D.; resources A.E., P.D., K.P.V. and R.D.R.; data curation C.P. and P.M.; writing—original draft preparation G.M.; writing—review and editing, P.D. and D.E.F.; supervision A.C. All authors have read and agreed to the published version of the manuscript.

Funding: This research received no external funding.

Institutional Review Board Statement: Not applicable.

Informed Consent Statement: Informed consent was obtained from the subjects.

Data Availability Statement: The data presented in this study are available upon request from the corresponding author. The data are not publicly available due to privacy issues.

Conflicts of Interest: The authors declare no conflict of interest.

Abbreviations

ANA	Antinuclear Antibodies
CD	Cluster of Differentiation
CRP	C-reactive Protein
CT	Computed Tomography
ED	Emergency Department
FDC	Follicular Dendritic Cell
HLH	Hemophagocytic Lymphohistiocytosis
INF α	Interferon Alpha
ISG	INF-stimulated genes
KFD	Kikuchi–Fujimoto disease
MFI	Mean Fluorescence Intensity
SSC	Side Scatter
SSc	Systemic Sclerosis
SIADs	Systemic Inflammatory Autoimmune Diseases
SIGLEC-1	Sialic Acid-Binding Ig-like Lectin 1
pDC	Plasmacytoid Dendritic Cell

References

1. Kikuchi, M. Lymphadenitis showing focal reticulum cell hyperplasia with nuclear debris and phagocytosis. *Nippon Ketsueki Gakkai Zasshi* **1972**, *35*, 379–380.
2. Fujimoto, Y.; Kozima, Y.; Yamaguchi, K. Cervical subacute necrotizing lymphadenitis. A new clinicopathological entity. *Naika* **1972**, *20*, 920–927.
3. Dumas, G.; Prendki, V.; Haroche, J.; Amoura, Z.; Cacoub, P.; Galicier, L.; Meyer, O.; Rapp, C.; Deligny, C.; Godeau, B.; et al. Kikuchi-Fujimoto disease: Retrospective study of 91 cases and review of the literature. *Medicine* **2014**, *93*, 372–382, Erratum in *Medicine* **2014**, *93*, 414. [[CrossRef](#)] [[PubMed](#)]
4. Zaccarelli, F.; de Vincentiis, M.; D’Erme, G.; Greco, A.; Natalucci, F.; Fusconi, M. Kikuchi-Fujimoto Disease: A Distinct Pathological Entity but also an “Overlap” Autoimmune Syndrome—A systematic review. *Curr. Rheumatol. Rev.* **2022**, *19*, 159–167. [[CrossRef](#)]
5. Pepe, F.; Disma, S.; Teodoro, C.; Pepe, P.; Magro, G. Kikuchi-Fujimoto disease: A clinicopathologic update. *Pathologica* **2016**, *108*, 120–129. [[PubMed](#)]
6. Pileri, S.A.; Facchetti, F.; Ascani, S.; Sabattini, E.; Poggi, S.; Piccioli, M.; Rondelli, D.; Vergoni, F.; Zinzani, P.L.; Piccaluga, P.P.; et al. Myeloperoxidase expression by histiocytes in Kikuchi’s and Kikuchi-like lymphadenopathy. *Am. J. Pathol.* **2001**, *159*, 915–924. [[CrossRef](#)] [[PubMed](#)]
7. Sukswai, N.; Jung, H.R.; Amr, S.S.; Ng, S.B.; Sheikh, S.S.; Lyapichev, K.; El Hussein, S.; Loghavi, S.; Agbay, R.L.M.C.; Miranda, R.N.; et al. Immunopathology of Kikuchi-Fujimoto disease: A reappraisal using novel immunohistochemistry markers. *Histopathology* **2020**, *77*, 262–274. [[CrossRef](#)] [[PubMed](#)]
8. Sato, H.; Asano, S.; Mori, K.; Yamazaki, K.; Wakasa, H. Plasmacytoid Dendritic Cells Producing Interferon- α (IFN- α) and Inducing Mx1 Play an Important Role for CD4(+) Cells and CD8(+) Cells in Necrotizing Lymphadenitis. *J. Clin. Exp. Hematop.* **2015**, *55*, 127–135. [[CrossRef](#)]
9. Lin, C.W.; Liu, T.Y.; Lin, C.J.; Hsu, S.M. Oligoclonal T cells in histiocytic necrotizing lymphadenopathy are associated with TLR9+ plasmacytoid dendritic cells. *Lab. Invest.* **2005**, *85*, 267–275. [[CrossRef](#)]
10. Tabata, T.; Takata, K.; Miyata-Takata, T.; Sato, Y.; Ishizawa, S.; Kunitomo, T.; Nagakita, K.; Ohnishi, N.; Taniguchi, K.; Noujima-Harada, M.; et al. Characteristic Distribution Pattern of CD30-positive Cytotoxic T Cells Aids Diagnosis of Kikuchi-Fujimoto Disease. *Appl. Immunohistochem. Mol. Morphol.* **2018**, *26*, 274–282. [[CrossRef](#)]
11. Kishimoto, K.; Tate, G.; Kitamura, T.; Kojima, M.; Mitsuya, T. Cytologic features and frequency of plasmacytoid dendritic cells in the lymph nodes of patients with histiocytic necrotizing lymphadenitis (Kikuchi-Fujimoto disease). *Diagn. Cytopathol.* **2010**, *38*, 521–526. [[CrossRef](#)] [[PubMed](#)]

12. Asano, S.; Sato, H.; Mori, K.; Yamazaki, K.; Naito, H.; Suzuki, H. Necrotizing lymphadenitis may be induced by overexpression of Toll-like receptor7 (TLR7) caused by reduced TLR9 transport in plasmacytoid dendritic cells (PDCs). *J. Clin. Exp. Hematop.* **2021**, *61*, 85–92. [[CrossRef](#)] [[PubMed](#)]
13. Li, E.Y.; Xu, J.; Nelson, N.D.; Teachey, D.T.; Tan, K.; Romberg, N.; Behrens, E.; Pillai, V. Kikuchi-Fujimoto disease is mediated by an aberrant type I interferon response. *Mod. Pathol.* **2022**, *35*, 462–469. [[CrossRef](#)] [[PubMed](#)]
14. York, M.R.; Nagai, T.; Mangini, A.J.; Lemaire, R.; van Seventer, J.M.; Lafyatis, R. A macrophage marker, Siglec-1, is increased on circulating monocytes in patients with systemic sclerosis and induced by type I interferons and toll-like receptor agonists. *Arthritis Rheum.* **2007**, *56*, 1010–1020, Erratum in *Arthritis Rheum.* **2007**, *56*, 1675. [[CrossRef](#)] [[PubMed](#)]
15. Zorn-Pauly, L.; von Stuckrad, A.S.L.; Klotsche, J.; Rose, T.; Kallinich, T.; Enghard, P.; Ostendorf, L.; Burns, M.; Doerner, T.; Meisel, C.; et al. Evaluation of SIGLEC1 in the diagnosis of suspected systemic lupus erythematosus. *Rheumatology* **2022**, *61*, 3396–3400. [[CrossRef](#)] [[PubMed](#)]
16. Graf, M.; von Stuckrad, S.L.; Uruha, A.; Klotsche, J.; Zorn-Pauly, L.; Unterwalder, N.; Buttgereit, T.; Krusche, M.; Meisel, C.; Burmester, G.R.; et al. SIGLEC1 enables straightforward assessment of type I interferon activity in idiopathic inflammatory myopathies. *RMD Open* **2022**, *8*, e001934. [[CrossRef](#)] [[PubMed](#)]
17. Lerkvaleekul, B.; Veldkamp, S.R.; van der Wal, M.M.; Schatorjé, E.J.H.; Kamphuis, S.S.M.; van den Berg, J.M.; Hissink Muller, P.C.E.; Armbrust, W.; Vastert, S.J.; Wienke, J.; et al. Siglec-1 expression on monocytes is associated with the interferon signature in juvenile dermatomyositis and can predict treatment response. *Rheumatology* **2022**, *61*, 2144–2155. [[CrossRef](#)] [[PubMed](#)]
18. Comins-Boo, A.; Gutiérrez-Larrañaga, M.; Roa-Bautista, A.; Guiral Foz, S.; Renuncio García, M.; González López, E.; Irure Ventura, J.; Fariñas-Álvarez, M.C.; San Segundo, D.; López Hoyos, M. Validation of a Quick Flow Cytometry-Based Assay for Acute Infection Based on CD64 and CD169 Expression. New Tools for Early Diagnosis in COVID-19 Pandemic. *Front. Med.* **2021**, *8*, 655785. [[CrossRef](#)]
19. Bourgoin, P.; Soliveres, T.; Ahriz, D.; Arnoux, I.; Meisel, C.; Unterwalder, N.; Morange, P.E.; Michelet, P.; Malergue, F.; Markarian, T. Clinical research assessment by flow cytometry of biomarkers for infectious stratification in an Emergency Department. *Biomark. Med.* **2019**, *13*, 1373–1386. [[CrossRef](#)]
20. Bedin, A.S.; Makinson, A.; Picot, M.C.; Mennechet, F.; Malergue, F.; Pisoni, A.; Nyiramigisha, E.; Montagnier, L.; Bollore, K.; Debieesse, S.; et al. Monocyte CD169 Expression as a Biomarker in the Early Diagnosis of Coronavirus Disease 2019. *J. Infect. Dis.* **2021**, *223*, 562–567, Erratum in *J. Infect. Dis.* **2022**, *225*, 744. [[CrossRef](#)]
21. van den Hoogen, F.; Khanna, D.; Fransen, J.; Johnson, S.R.; Baron, M.; Tyndall, A.; Matucci-Cerinic, M.; Naden, R.P.; Medsger, T.A., Jr.; Carreira, P.E.; et al. 2013 classification criteria for systemic sclerosis: An American College of Rheumatology/European League against Rheumatism collaborative initiative. *Arthritis Rheum.* **2013**, *65*, 2737–2747. [[CrossRef](#)] [[PubMed](#)]
22. Wang, W.; Huang, S.; Nong, L.; Li, X.; Li, D.; Zhang, B.; Li, T. Clinicopathologic Analysis of Kikuchi-Fujimoto Disease and Etiologic Exploration Using Metagenomic Next-Generation Sequencing. *Arch. Pathol. Lab. Med.* **2022**, *147*, 767–773. [[CrossRef](#)] [[PubMed](#)]
23. Ikeda, K.; Kakehi, E.; Adachi, S.; Kotani, K. Kikuchi-Fujimoto disease following SARS-CoV-2 vaccination. *BMJ Case Rep.* **2022**, *15*, e250601. [[CrossRef](#)] [[PubMed](#)]
24. Wiśniewska, K.; Pawlak-Buś, K.; Leszczyński, P. Kikuchi-Fujimoto disease associated with primary Sjögren’s syndrome—Literature review based on a case report. *Reumatologia* **2020**, *58*, 251–256. [[CrossRef](#)] [[PubMed](#)]
25. Fernandes, B.M.; Bernardes, M.; Barroca, H.; Costa, L. Kikuchi-Fujimoto Disease Associated With Mixed Connective Tissue Disease: A Late Recurrence Case. *J. Clin. Rheumatol.* **2021**, *27*, S779–S780. [[CrossRef](#)] [[PubMed](#)]
26. Garcia-Zamalloa, A.; Taboada-Gomez, J.; Bernardo-Galán, P.; Magdalena, F.M.; Zaldumbide-Dueñas, L.; Ugarte-Maiztegui, M. Bilateral pleural effusion and interstitial lung disease as unusual manifestations of Kikuchi-Fujimoto disease: Case report and literature review. *BMC Pulm. Med.* **2010**, *10*, 54. [[CrossRef](#)] [[PubMed](#)]
27. De Stefano, P.; Chizzolini, C.; Lalive, P.H.; Lascano, A.M. Limbic encephalitis associated with systemic sclerosis. *Mult. Scler. Relat. Disord.* **2018**, *24*, 142–144. [[CrossRef](#)]
28. Shabana, M.; Warnack, W. An atypical neurologic complication of Kikuchi-Fujimoto Disease. *Neurol. Neuroimmunol. Neuroinflamm.* **2020**, *7*, e707. [[CrossRef](#)]
29. Gism Elseed, I.; Osman, H.; Ahmedfiqi, O.; Najmi, F.; Al-Hebshi, A. Kikuchi-Fujimoto Disease: A Rare Benign Cause of Lymphadenopathy That Mimics Malignant Lymphoma. *Cureus* **2022**, *14*, e23177. [[CrossRef](#)]
30. Yu, F.; Ba, X.; Yang, H.; Huang, K.; Zhang, Y.; Zhang, H.; Xu, L.; Wang, J.; Wang, L.; Wang, Z.; et al. Kikuchi disease with an exuberant proliferation of large T-cells: A study of 25 cases that can mimic T-Cell lymphoma. *Histopathology* **2023**, *82*, 340–353. [[CrossRef](#)]
31. Jaffe, E. (Ed.) PART II • Normal and Reactive Conditions of Hematopoietic Tissues, Kikuchi’s Lymphadenitis. In *Hematopathology*, 2nd ed.; Elsevier: Philadelphia, PA, USA, 2017.
32. Perry, A.M.; Choi, S.M. Kikuchi-Fujimoto Disease: A Review. *Arch. Pathol. Lab. Med.* **2018**, *142*, 1341–1346. [[CrossRef](#)] [[PubMed](#)]
33. Ohshima, K.; Shimazaki, K.; Kume, T.; Suzumiya, J.; Kanda, M.; Kikuchi, M. Perforin and Fas pathways of cytotoxic T-cells in histiocytic necrotizing lymphadenitis. *Histopathology* **1998**, *33*, 471–478. [[CrossRef](#)] [[PubMed](#)]
34. Nelson, N.D.; Meng, W.; Rosenfeld, A.M.; Bullman, S.; Sekhar Peadamallu, C.; Nomburg, J.L.; Wertheim, G.B.; Paessler, M.E.; Pinkus, G.; Hornick, J.L.; et al. Characterization of Plasmacytoid Dendritic Cells, Microbial Sequences, and Identification of a Candidate Public T-Cell Clone in Kikuchi-Fujimoto Disease. *Pediatr. Dev. Pathol.* **2021**, *24*, 193–205. [[CrossRef](#)] [[PubMed](#)]

35. Pilichowska, M.E.; Pinkus, J.L.; Pinkus, G.S. Histiocytic necrotizing lymphadenitis (Kikuchi-Fujimoto disease): Lesional cells exhibit an immature dendritic cell phenotype. *Am. J. Clin. Pathol.* **2009**, *131*, 174–182. [[CrossRef](#)] [[PubMed](#)]
36. Scott, G.D.; Kumar, J.; Oak, J.S.; Boyd, S.D.; Raess, P.W.; Gratzinger, D.A. Histology-Independent Signature Distinguishes Kikuchi-Fujimoto Disease/Systemic Lupus Erythematosus-Associated Lymphadenitis From Benign and Malignant Lymphadenopathies. *Am. J. Clin. Pathol.* **2020**, *154*, 215–224. [[CrossRef](#)] [[PubMed](#)]
37. Yu, S.C.; Huang, H.H.; Chen, C.N.; Chen, T.C.; Yang, T.L. Blood cell and marrow changes in patients with Kikuchi disease. *Haematologica* **2022**, *107*, 1981–1985. [[CrossRef](#)] [[PubMed](#)]
38. Zhang, R.; Liang, L.; Li, D.; Bai, Y.; Li, X. Analysis of the clinical manifestations and 18F-FDG PET-CT findings in 40 patients with histiocytic necrotizing lymphadenitis. *Medicine* **2021**, *100*, e27189. [[CrossRef](#)]
39. Ishimura, M.; Yamamoto, H.; Mizuno, Y.; Takada, H.; Goto, M.; Doi, T.; Hoshina, T.; Ohga, S.; Ohshima, K.; Hara, T. A non-invasive diagnosis of histiocytic necrotizing lymphadenitis by means of gene expression profile analysis of peripheral blood mononuclear cells. *J. Clin. Immunol.* **2013**, *33*, 1018–1026. [[CrossRef](#)]
40. Yılmaz, U.; Güner, S.; Eşkazan, T.; Demiröz, A.S.; Kurtuluş, G.; Bahar, F.; Uğurlu, S.; Eşkazan, A.E. Kikuchi Fujimoto disease as the presenting component of VEXAS syndrome: A case report of a probable association. *Clin. Rheumatol.* **2022**, *41*, 3589–3592. [[CrossRef](#)]
41. Lee, S.M.S.; Fan, B.E.; Lim, J.H.; Goh, L.L.; Lee, J.S.S.; Koh, L.W. A case of VEXAS syndrome manifesting as Kikuchi-Fujimoto disease, relapsing polyarthritides, venous thromboembolism and macrocytic anaemia. *Rheumatology* **2021**, *60*, e304–e306. [[CrossRef](#)]
42. Prenzler, S.; Rudrawar, S.; Waespy, M.; Kelm, S.; Anoopkumar-Dukie, S.; Haselhorst, T. The role of sialic acid-binding immunoglobulin-like-lectin-1 (siglec-1) in immunology and infectious disease. *Int. Rev. Immunol.* **2023**, *42*, 113–138. [[CrossRef](#)] [[PubMed](#)]
43. Cai, K.; Chen, Q.; Shi, D.; Huang, S.; Wang, C.; Ai, Z.; Jiang, J. Sialylation-dependent interaction between PD-L1 and CD169 promotes monocyte adhesion to endothelial cells. *Glycobiology* **2023**, *33*, 215–224. [[CrossRef](#)] [[PubMed](#)]
44. Affandi, A.J.; Olesek, K.; Grabowska, J.; Nijen Twilhaar, M.K.; Rodríguez, E.; Saris, A.; Zwart, E.S.; Nossent, E.J.; Kalay, H.; de Kok, M.; et al. CD169 Defines Activated CD14⁺ Monocytes With Enhanced CD8⁺ T Cell Activation Capacity. *Front. Immunol.* **2021**, *12*, 697840. [[CrossRef](#)] [[PubMed](#)]
45. Sakumura, N.; Yokoyama, T.; Usami, M.; Hosono, Y.; Inoue, N.; Matsuda, Y.; Tasaki, Y.; Wada, T. CD169 expression on monocytes as a marker for assessing type I interferon status in pediatric inflammatory diseases. *Clin. Immunol.* **2023**, *250*, 109329. [[CrossRef](#)] [[PubMed](#)]
46. Grabowska, J.; Lopez-Venegas, M.A.; Affandi, A.J.; den Haan, J.M.M. CD169⁺ Macrophages Capture and Dendritic Cells Instruct: The Interplay of the Gatekeeper and the General of the Immune System. *Front. Immunol.* **2018**, *9*, 2472. [[CrossRef](#)] [[PubMed](#)]
47. Gkirtzimanaki, K.; Kabrani, E.; Nikoleri, D.; Polyzos, A.; Blanas, A.; Sidiropoulos, P.; Makrigiannakis, A.; Bertias, G.; Boumpas, D.T.; Verginis, P. IFN α Impairs Autophagic Degradation of mtDNA Promoting Autoreactivity of SLE Monocytes in a STING-Dependent Fashion. *Cell Rep.* **2018**, *25*, 921–933. [[CrossRef](#)]
48. Caielli, S.; Cardenas, J.; de Jesus, A.A.; Baisch, J.; Walters, L.; Blanck, J.P.; Balasubramanian, P.; Stagnar, C.; Ohouo, M.; Hong, S.; et al. Erythroid mitochondrial retention triggers myeloid-dependent type I interferon in human SLE. *Cell* **2021**, *184*, 4464–4479.e19. [[CrossRef](#)]
49. Trombetta, A.C.; Soldano, S.; Contini, P.; Tomatis, V.; Ruaro, B.; Paolino, S.; Brizzolara, R.; Montagna, P.; Sulli, A.; Pizzorni, C.; et al. A circulating cell population showing both M1 and M2 monocyte/macrophage surface markers characterizes systemic sclerosis patients with lung involvement. *Respir. Res.* **2018**, *19*, 186. [[CrossRef](#)]
50. Hénauld, J.; Robitaille, G.; Sénécal, J.L.; Raymond, Y. DNA topoisomerase I binding to fibroblasts induces monocyte adhesion and activation in the presence of anti-topoisomerase I autoantibodies from systemic sclerosis patients. *Arthritis Rheum.* **2006**, *54*, 963–973. [[CrossRef](#)]
51. Schneider, L.; Marcondes, N.A.; Hax, V.; da Silva Moreira, I.F.; Ueda, C.Y.; Piovesan, R.R.; Xavier, R.; Chakr, R. Flow cytometry evaluation of CD14/CD16 monocyte subpopulations in systemic sclerosis patients: A cross sectional controlled study. *Adv. Rheumatol.* **2021**, *61*, 27. [[CrossRef](#)]
52. Höppner, J.; Casteleyn, V.; Biesen, R.; Rose, T.; Windisch, W.; Burmester, G.R.; Siegert, E. SIGLEC-1 in Systemic Sclerosis: A Useful Biomarker for Differential Diagnosis. *Pharmaceuticals* **2022**, *15*, 1198. [[CrossRef](#)]
53. Marmey, B.; Boix, C.; Barbaroux, J.B.; Dieu-Nosjean, M.C.; Diebold, J.; Audouin, J.; Fridman, W.H.; Mueller, C.G.; Molina, T.J. CD14 and CD169 expression in human lymph nodes and spleen: Specific expansion of CD14⁺CD169[–] monocyte-derived cells in diffuse large B-cell lymphomas. *Hum. Pathol.* **2006**, *37*, 68–77. [[CrossRef](#)]

Disclaimer/Publisher’s Note: The statements, opinions and data contained in all publications are solely those of the individual author(s) and contributor(s) and not of MDPI and/or the editor(s). MDPI and/or the editor(s) disclaim responsibility for any injury to people or property resulting from any ideas, methods, instructions or products referred to in the content.